

# Implementing LoRa MIMO System for Internet of Things

Atonu Ghosh, *Graduate Student Member, IEEE*, Sharath Chandan, Sudip Misra, *Fellow, IEEE*

arXiv:2501.07148v1 [cs.CY] 13 Jan 2025

**Abstract**—Bandwidth constraints limit LoRa implementations. Contemporary IoT applications require higher throughput than that provided by LoRa. This work introduces a LoRa Multiple Input Multiple Output (MIMO) system and a spatial multiplexing algorithm to address LoRa’s bandwidth limitation. The transceivers in the proposed approach modulate the signals on distinct frequencies of the same LoRa band. A Frequency Division Multiplexing (FDM) method is used at the transmitters to provide a wider MIMO channel. Unlike conventional Orthogonal Frequency Division Multiplexing (OFDM) techniques, this work exploits the orthogonality of the LoRa signals facilitated by its proprietary Chirp Spread Spectrum (CSS) modulation to perform an OFDM in the proposed LoRa MIMO system. By varying the Spreading Factor (SF) and bandwidth of LoRa signals, orthogonal signals can transmit on the same frequency irrespective of the FDM. Even though the channel correlation is minimal for different spreading factors and bandwidths, different Carrier Frequencies (CF) ensure the signals do not overlap and provide additional degrees of freedom. This work assesses the proposed model’s performance and conducts an extensive analysis to provide an overview of resources consumed by the proposed system. Finally, this work provides the detailed results of a thorough evaluation of the model on test hardware.

**Index Terms**—Internet of Things (IoT), LoRa Throughput, Spatial-multiplexing (SM), LoRa MIMO, Multiple Input Multiple Output (MIMO), Quality-of-Service (QoS).

## I. INTRODUCTION

LoRa has found a wide range of applications, including wide adoption in industries due to its low power and extended range capabilities [1]–[4]. IoT devices are battery-powered, and LoRa enables longer system lifetime with a trade-off on data rates and payload size [5], [6]. The compromised throughput in LoRa implementations makes it unsuitable for time-sensitive use cases. Therefore, it is essential to enhance the throughput of the LoRa system [7], [8]. LoRa has become one of the front-runners in Industrial Internet of Things (IIoT) deployments [9]. There is a notable surge in interest in LoRa. Integrating MIMO provides better capacity along with Multiple Antenna (MA) techniques [10]. LoRa is one of the principal beneficiaries of MIMO. The metamorphosis of LoRa is significant in achieving more mature IoT implementations, and sophisticated signal processing algorithms are vital in improving the system’s performance. Nevertheless, the makers must consider resource constraints to devise an energy-efficient communication technique.

Atonu Ghosh and Sudip Misra are with the Department of Computer Science and Engineering, Indian Institute of Technology Kharagpur, Kharagpur 721302, India (e-mail: atonughosh@outlook.com; sudip\_misra@yahoo.com).

Sharath Chandan is with the Department of Electronics and Communication Engineering at the Sona College of Technology, Salem 636005, Tamil Nadu, India (e-mail: sharathchandan5@yahoo.com).

The article employs several approaches to improve the system’s throughput. It proposes a Frequency Division Multiplexing (FDM) scheme to enhance spectral efficiency by utilizing four frequencies of the same spectrum. The system performs FDM with four Single Input Single Output (SISO) links to construct a 4X4 MIMO channel and evaluate the channel metrics. The signals modulate on specific carrier frequencies on different spreading factors and bandwidth combinations to provide orthogonality. The channel correlation is almost absent, while the symbols are orthogonal. It allows the transmission of signals on the same carrier frequency. However, the uncorrelated propagation of parallel signals is enhanced using characteristic frequency sub-channels. The antenna diversity equips the system with the flexibility to perform spatial processing at the receiver, boosting the system’s data throughput. The article assesses a sophisticated spatial multiplexing approach to attain MIMO gain to increase the data rate. Higher data rates are critical in modern IoT applications, enabling enhanced Quality-of-service (QoS). The Bit Error Rate (BER) demonstrates the system’s data reliability. The Signal to Noise Ration (SNR) and Received Signal Strength Indicator (RSSI) assist in assessing the system’s throughput. MA techniques with suitable signal processing methods, such as spatial multiplexing, deliver the multiplexing gain, increasing the system’s throughput. The Spatial Multiplexing (SM) technique necessitates appropriate signal processing techniques to effectively channel the independent data streams. Performing singular value decomposition for a 4x4 MIMO matrix helps derive the feasible number of distinct streams that can be transmitted simultaneously. Precoding is essential since prior knowledge of the channel characteristics simplifies the computational functionality of the system.

### A. Motivation

In recent years, the number of IoT devices has grown exponentially, which necessitates the development of appropriate communication technologies to handle massive amounts of data. Additionally, critical applications such as industrial setups require quality of service (QoS) requirements to be met. Towards this, there have been considerable efforts in utilizing multiple antenna systems by integrating MIMO technology with various wireless communication systems. However, there is still a need for more effective methods to maximize the throughput without compromising the spectrum. With bandwidth being a limited resource, it is essential to use it wisely to maximize available resources. There has never been a justification for not using several antennas on either section

of the communication system to achieve better throughput. Moreover, while the upfront costs of purchasing additional hardware for MIMO implementation are high, the potential benefits of increased bandwidth and spectral efficiency can outweigh these costs in the long run.

Furthermore, MIMO technologies are highly versatile and can be applied to various data transfer mechanisms, making them a valuable technique for wireless communication systems. Therefore, there is a need for further research to integrate MIMO technology for different communication techniques, such as LoRa, to maximize available bandwidth. LoRa suffers from low data rates since it is a low-power, long-range communication technique. We aim to explore the potential of MIMO technology in LoRa-based communication systems and its ability to enhance data transfer rates while making the best use of available resources. This study paves the way for developing new and more effective methods for MIMO implementation, leading to significant advancements in wireless communication technology. Suitable signal processing algorithms allow better performance in existing systems. The strategy's general applicability to a variety of data transfer mechanisms proves to be valuable.

### B. Contributions

The LoRa MIMO system is an end-to-end, highly scalable, unaided, and efficient approach. The system's architecture is ruminative, making it suitable for various applications. Henceforth, it reduces transmission and reception latency. Furthermore, preprocessing of the data provides prudent utilization of the bandwidth. It helps attain a higher throughput of raw data. It provides scope to send compressed data and transmit larger payloads. The distinctive features of this work are as follows.

- 1) This work proposes an end-to-end LoRa-MIMO system for improved data capacity requirements in industrial IoT deployments. Besides, it discusses the system features and its functioning elaborately.
- 2) The actual hardware-based 4x4 MIMO system deployment observations are discussed in detail. Furthermore, this work analyses the performance of the test hardware and presents the performance metrics in terms of execution time, memory usage, latency, and power consumption.
- 3) This work uses various channel characteristics to present results for varied bandwidth, coding rate, and spreading factors to test the spatially multiplexed channel. Mathematical tools aid the simulation of the proposed system, validate the model on test hardware, and present the comparative outcomes.

## II. RELATED WORK

Due to the inherent characteristics of long-range and low power consumption, it has gained considerable research initiatives in recent years. Moreover, as the LoRa networks suffer from the problem of low bandwidth, it has attracted fresh efforts towards bandwidth enhancement.

Researchers proposed a mathematical model to demonstrate the correlation between the SF and data rates. They simulated the model to prove its effectiveness and concluded that increasing the SF gives broader coverage with reduced data rates [11]. Furthermore, a group of researchers proposed an algorithm for allocating SF in the clusters of a multi-hop LoRa network. The proposed algorithms considered the time on air while transferring data between subnets [12]. In another work, the authors proposed implementing an Interleaved Chirp Spreading LoRa (ICS-LoRa) modulation-based parallel network. They attributed the increase in the network capacity in such an arrangement to the cross-correlation between the ICS-LoRa and the official LoRa [13]. Additionally, researchers have proposed an incentive-based game theoretic approach for allocating the SFs such that the interference is minimized and higher bandwidth is achieved [14]. Another group of researchers proposed a model to calculate the SF allocation time in LoRa networks and considered the service requirements of the nodes in the network. They proposed algorithms and implemented them in their system [15]. Researchers have also demonstrated the correlation between the SFs, interference, and collisions. They concluded that when higher SFs are assigned to far-flung devices, the performance is not guaranteed [16]. Finally, the works in the literature also concluded that the Inter-SF interference is null using different bandwidths for the same spreading factor [17]–[20].

“CharIoT”, a distributed MIMO receiver system for low-power IoT networks, was proposed by a group of researchers. The proposed system received signals from IoT gateways and forwarded them to the cloud. The system helped avoid collisions of low-power IoT devices operating at sub-1GHz ISM bands [21]. Additionally, researchers have proposed several MIMO systems and their coding schemes. A LoRa MIMO system was proposed, and numerical simulation was performed on a point-to-point communication link to express the enhancement in the data rate. The authors considered a transmitter and a receiver with multiple antennas in their work [22]. A similar work proposed a “Space-Time Block Coding (STBC)” MIMO system. The researchers provided a detailed model of the proposed system and evaluated the results. They analyzed the throughput of the proposed system and concluded that their model was superior [23]. However, the LoRa MIMO systems proposed and evaluated thus far are simulation-based and do not provide actual hardware-based implementation and analysis.

Moreover, researchers have put significant efforts into enhancing LoRa link capacity. In a prior work, the authors experimented with the scalability of LoRa solutions. They further developed a prototype to test in crowded environments [24]. Furthermore, strategies involving the Spreading Factor (SF) have been proven to enhance connectivity in LoRa systems, as suggested in [25]. To enable parallel transmission in LoRa uplink systems, authors proposed an energy-efficient and adaptive scheme for virtual MIMO transmission. They formulated a maximization problem to optimize the end devices' power and spreading factor. They also simulated the proposed system, and their results confirmed the superiority of the scheme [26]. Finally, the researchers in [27] experimented

with the hardware implementation of a LoRa gateway with two antennas. They achieved a throughput of 4.6 kbps.

**Synthesis:** The salient features of LoRa have drawn attention from the research community and have been widely adopted. Numerous efforts have been put in lately to further enhance the capabilities of LoRa, specifically to enhance the bandwidth. However, a majority of these works are theoretical and simulation-based. There is a lack of a system and methods for an end-to-end LoRa MIMO system suitable for dense IoT deployments.

### III. SYSTEM MODEL AND DESCRIPTION

LoRa's CSS modulation scheme does frequency shifting. In this scheme, the bit rate varies linearly with the channel's bandwidth. The coding rate of LoRa characterizes the information carrying bits of the transmitted data. If CR = 4/5, an extra bit is assigned for error correction. The signal is error-free for higher coding rates but provides low data rates. For a striking balance between data rate and signal integrity, the CR of 4/5 and 4/6 can be used. The spreading factor specifies the range of the transmission channel. In line-of-sight communication, for higher spreading factors, the coverage ranges across several hundred kilometers but with lower data rates. So, a spreading factor of 6,7 is suitable for a shorter range and a higher throughput.

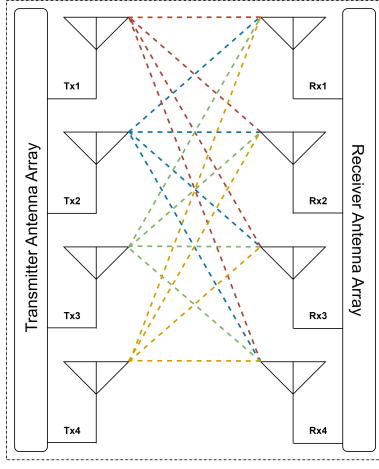


Figure 1. Four Transmitter and Four Receiver (4T4R) SM MIMO channel

The receive-transmit relationship of the proposed LoRa MIMO system is depicted in Fig. 1 and can be mathematically represented as

$$\rho = H\Gamma + \omega_i \quad (1)$$

where  $\rho$ ,  $\Gamma$  are the receive and transmit vectors,  $H$  represents the Channel Matrix of the MIMO channel, and  $\omega_i$  represents the White Gaussian noise for  $i^{th}$  channel. The channel matrix is also denoted by  $(\mu)$  as a  $p \times q$  matrix, where  $p = q = 4$ .

$$\mu = [\mu_{pq}] \quad (2)$$

Hence, by Eq. 1, the receive vector of the MIMO channel is represented as

$$[\rho_i] = [\mu_{pq}] \times [\Gamma_i] + [\omega_i] \quad (3)$$

The product of the Channel Matrix in Eq. 1 and the transmit vector, along with the White Gaussian noise, gives the receive vector.

The channel matrix's Singular Value Decomposition (SVD) gives us the maximum number of possible spatial streams to be transmitted through a MIMO channel. We evaluate the SVD of the channel matrix by decomposing the Channel Matrix  $H$ . The channel is decomposed such that  $H$  is a product of three matrices  $U$ ,  $\Sigma$ , and  $V^H$ . The receive vector is given by

$$\rho = U\Sigma V^H \Gamma + \omega_i \quad (4)$$

In the above equation, the channel matrix is substituted with  $H = U\Sigma V^H$  in the input-output relationship of the MIMO channel in Eq. 1. The  $\Sigma$  is a diagonal matrix of non-negative singular values where the matrix  $U$  and the Hermitian of the  $U$  matrix  $U^H$  have the following properties  $U^H U = I$ , where  $I$  is the identity matrix. Similarly,  $V^H V = VV^H = I$ . The receive vector is multiplied with  $U^H$  on both sides of the equation to obtain the net system model. It is a post-processing technique since the receive vector is modified as a product of the Hermitian of the matrix  $V$ .

$$\begin{aligned} U^H \rho &= U^H (U\Sigma V^H \Gamma + \omega_i) \\ \tilde{\rho} &= U^H U \Sigma V^H \Gamma + U^H \omega_i \\ \tilde{\rho} &= \Sigma V^H \Gamma + \tilde{\omega}_i \end{aligned} \quad (5)$$

The precoding of the transmitted vector enables superior connectivity between the transmitter and receiver of the spatially multiplexed system. It provides system resilience by exchanging channel knowledge with the transmitter. Since the configuration is symmetrical, we obtain the channel knowledge of the system by

$$\begin{aligned} \Gamma &= V\tilde{\Gamma} \\ \tilde{\rho} &= \Sigma V^H V\tilde{\Gamma} + \tilde{\omega}_i \\ \tilde{\rho} &= \Sigma\tilde{\Gamma} + \tilde{\omega}_i \end{aligned} \quad (6)$$

The SVD of the channel matrix is given by

$$\begin{bmatrix} \tilde{\rho}_1 \\ \tilde{\rho}_2 \\ \tilde{\rho}_3 \\ \tilde{\rho}_4 \end{bmatrix} = \begin{bmatrix} \sigma_1 & 0 & 0 & 0 \\ 0 & \sigma_2 & 0 & 0 \\ 0 & 0 & \sigma_3 & 0 \\ 0 & 0 & 0 & \sigma_4 \end{bmatrix} \times \begin{bmatrix} \tilde{\Gamma}_1 \\ \tilde{\Gamma}_2 \\ \tilde{\Gamma}_3 \\ \tilde{\Gamma}_4 \end{bmatrix} + \begin{bmatrix} \omega_1 \\ \omega_2 \\ \omega_3 \\ \omega_4 \end{bmatrix} \quad (7)$$

The four discrete spatial streams of the received vectors with their respective transmit vectors, along with infinitesimally minimal noise, are

$$\tilde{\rho}_1 = \sigma\tilde{\Gamma}_1 + \tilde{\omega}_1 \quad (8)$$

$$\tilde{\rho}_2 = \sigma\tilde{\Gamma}_2 + \tilde{\omega}_2 \quad (9)$$

$$\tilde{\rho}_3 = \sigma\tilde{\Gamma}_3 + \tilde{\omega}_3 \quad (10)$$

$$\tilde{\rho}_4 = \sigma\tilde{\Gamma}_4 + \tilde{\omega}_4 \quad (11)$$

The SVD of the 4x4 channel matrix  $\mu$  decomposes the matrix into four spatially independent channels. The non-zero singular vectors of the matrix are the eigen-channels characterizing each data stream. This work interprets the

MIMO channel as parallel SVD SISO sub-channels with non-zero gains.

### A. Transmitter

The transmitter unit of the proposed LoRa MIMO system consists of four LoRa modules integrated to work in concert. It includes two microcontrollers that control a pair of LoRa modules. Each radio channel has a frequency assigned to communicate with the destination unit over four antennas, one for each LoRa module, thus forming a multi-antenna system. For each subsequent communication, the unit groups the packets to be sent into sets of four. It accomplishes the simultaneous transmission of four independent data streams by executing Algorithm 1.

### B. Receiver

The setup of the receiver unit is similar to that of the transmitter module. Four LoRa modules are connected and synchronized by the two microcontrollers. It also includes four antennas, one for each LoRa module. The antennas receive the chunks of data sent by the transmitter of corresponding frequencies. All the receiver modules in the receiver unit receive the data concurrently. The distinct packet IDs enable the reassembling of data chunks to retrieve the original message. The thread function in the master-slave microcontroller setup ensures that all the LoRa transceivers operate concurrently. The receiver unit's operation is outlined by Algorithm 2.

### C. Co-processor Configuration

Each transmitter and receiver of the proposed system interfaces two microcontrollers to operate four LoRa modules and perform data processing, transmission, and reception tasks. The two microcontrollers communicate and synchronize in a master-slave fashion over UART to form a single unit. The master microcontroller performs the initialization of the radio modules and handles calculations of the number of packets to be transmitted in the transmitter. The slave sender listens over UART for the data and sends them through its LoRa radio modules. The LoRa radio interacts with the microcontrollers through the SPI protocol. In the receiver unit, the same master-slave microcontrollers handle the initialization of radios, reception of message chunks, and reassembly of the messages. Thus, the proposed system executes the 4x4 MIMO SVD operation. Each microcontroller in the receiver and transmitter executes two independent threads, i.e., four threads in each unit.

### D. Message Processing

The transmitter threads calculate the data chunks needed to be transmitted. The sliced packets are equal to  $N$ , corresponding to the number of transmitter modules, i.e.,  $N = 4$  in this implementation. The sender calculates the number of chunks, forms batches of four packets for every transmission, and notifies the receiver unit of the number of chunks to be received. The two threads on the receiver unit receive the data and assemble the message based on the packet IDs as sent

---

### Algorithm 1 Transmission algorithm for LoRa MIMO system

#### Initialization:

- 1: Initialize the LoRa modules  $l_1, l_2, l_3$ , and  $l_4$
- 2: The frequencies are such that  $f_1 < f_2 < f_3 < f_4$
- 3: Establish UART to the slave MCU

#### Preprocessing:

- 4: Read the data  $I$  to be transmitted and slice the data such that  $i_1 = i_2 = i_3 = i_4$
- 5: Assign packet ID for identifying the packets while receiving and notify the receiver of the number of chunks through LoRa

#### Transmission:

- 6: **if**  $i = 4$  **then**
- 7:    $uart.write(i_n)$  ▷ where  $n = 2$
- 8:    $thread(send.l_1)$
- 9:    $thread(send.l_2)$
- 10: **else**
- 11:   **if**  $i > 2$  **then**
- 12:      $uart.write(i_n)$  ▷ where  $n = 1$
- 13:      $thread(send.l_1)$
- 14:      $thread(send.l_2)$
- 15:   **else if**  $i = 2$  **then**
- 16:      $thread(send.l_1)$
- 17:      $thread(send.l_2)$
- 18:   **else if**  $i = 1$  **then**
- 19:      $thread(send.l_1)$
- 20:   **end if**
- 21: **end if**

#### Reception:

- 22: **if**  $i = 2$  **then**
- 23:    $uart.read(i_n)$  ▷ where  $n = 2$
- 24:    $thread(send.l_3)$
- 25:    $thread(send.l_4)$
- 26: **else**
- 27:   **if**  $i = 1$  **then**
- 28:      $uart.read(i_n)$  ▷ where  $n = 1$
- 29:      $thread(send.l_3)$
- 30:   **else if**  $i = 0$  **then**
- 31:      $uart.read(i_n)$  ▷ listen over UART for data
- 32:   **end if**
- 33: **end if**

---

by the transmitter unit. The algorithms in the receiver and transmitter units thus slice the data into four pieces of equal size and transmit them concomitantly to conduct a spatially multiplexed 4T4R communication.

## IV. EXPERIMENTAL SETUP

The implementation of the proposed system's transmitter and receiver units consists of four RFM95W LoRa modules in each of them. Each unit consists of two ESP32 microcontrollers that form a master-slave configuration as explained in Sections III-A and III-B. As mentioned in Section III, each LoRa module has its own antenna; thus, each unit consists of four antennas. The antennas configured in this model are

---

**Algorithm 2** Receiver algorithm for LoRa MIMO system

---

**Initialization:**

- 1: Initialize the LoRa receiver modules  $l_5$ ,  $l_6$ ,  $l_7$ , and  $l_8$
- 2: The frequencies are such that  $f_5 < f_6 < f_7 < f_8$  where  $f_1 = f_5$ ,  $f_2 = f_6$ ,  $f_3 = f_7$ , and  $f_4 = f_8$
- 3: Establish UART to the Master MCU
- 4: By using the specified frequency of the corresponding sender, detect the data sent through LoRa

**Reception:**

```

5: if  $i = 2$  then
6:   thread(recv.l7)
7:   thread(recv.l8)
8:   uart.write(in)                                 $\triangleright$  where  $n = 2$ 
9: else if  $i = 1$  then
10:  thread(recv.l7)
11:  thread(recv.l8)
12:  uart.write(in)                                 $\triangleright$  where  $n = 1$ 
13: end if

```

**Data Processing:**

```

12: if  $i = 2$  then
13:   thread(recv.l1)
14:   thread(recv.l2)
15:   uart.read(in)                                 $\triangleright$  where  $n \leq 2$ 
16: else if  $i = 1$  then
17:   thread(send.l1)
18:   uart.read(in)
19: end if
20: for  $i = n$  do
21:   Post-processing of data
22: end for

```

---

compatible with LoRa frequencies of 868MHz and 915MHz, allowing the system to perform spatial multiplexing. The experimental setup configuration is presented in Table IV. This work's implementation of the proposed LoRa MIMO system is depicted in Fig. 2. The MIMO system is identical for both the transmitter and receiver.

Table I  
CONFIGURATIONS OF EXPERIMENT

#	Criterion	Value
1	Deployment type	MIMO
2	Microcontroller	ESP32
3	LoRa module	RFM95W
4	Firmware	MicroPython
5	LoRa Frequency	868MHz
6	LoRa Tx Power	20dBm
7	No. of Transmitters (Tx)	4
8	No. of Receivers (Rx)	4
9	No. of Hops	1

## V. PERFORMANCE EVALUATION

### A. Delay

1) *Transmission Delay*: The transmitter was set up to send 240 bytes of data to the receiver unit to calculate the average transmission delay. The LoRa modules with a link data rate of 37.5 kbps experimented in ten rounds and had an average



Figure 2. MIMO Hardware Setup

transmission delay of 67 ms. The LoRa module with 18.75 kbps throughput showed an average delay of 125 ms. The average trip times for 21.875 kbps, and 12.50 kbps data rates were observed to be 112 ms and 197 ms, respectively. The results of the observations are depicted in Fig. 3.

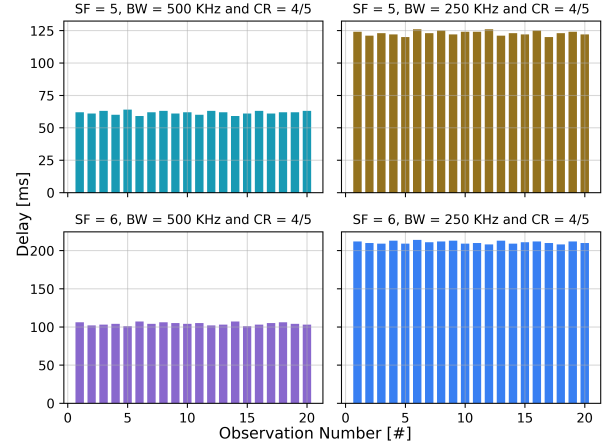


Figure 3. Round-trip times for varying spreading factor and bandwidth

2) *Receiving Delay*: The subsequent payloads for every two packets at the receiver have an infinitesimally slight delay of 21 milliseconds, while the other two packets are received simultaneously.

### B. Data Rate

The bitrate of the single LoRa channel using the  $\beta_r$  function in Eq. 12 gives the data rate. The heightened channel

width and lower spreading factors deliver increased bit rates. Altering these two parameters for the individual streams of the MIMO system gives orthogonality for interference-free transmission. We then verify the calculated data rate with the actual throughput of the MIMO system comprising four identical SISO channels.

The Bitrate for each SISO link is expressed as:

$$\beta_r = SF \times \frac{\left(\frac{4}{4+CR}\right)}{\left(\frac{2^SF}{BW}\right)}$$

$$\beta_r = \frac{4 \times SF \times BW}{(4 + CR) \times 2^SF} \quad (12)$$

where  $SF, CR$ , and  $BW$  are the Spreading Factor, Coding Rate, and Bandwidth, respectively.

Using the MIMO system's decomposed spatial channels, the effective data rate is the summation of the bit rates of the four individual SISO links. Accordingly, the data rate for any  $4 \times 4$  MIMO system with identical channel characteristics is the quadrupled value of the SISO data rate. A minimum coding rate enables taller data speeds since the ratio of information bits is higher than the redundant bits. Further, the latency is drastically less for a lower coding rate. So  $4/5$  is suited for scenarios demanding high throughput.

### C. Throughput

The maximum data rate of a single SISO link is around 37.5 kbps. In this article, the system uses a combination of four orthogonal channels. Figure 4 depicts the data rates of the independent channels observed, which are 36 Kb/s, 20.25 Kb/s, 18 Kb/s, and 11 Kb/s, respectively. The system's throughput ( $\beta$ ) is estimated for the spreading factors 6, 7, and 8 since they provide higher data rates. The internal buffer of the LoRa module is filled with the payload and transmitted. The transmission time and the number of packets sent are used to evaluate the throughput of the transmitter. As detailed in Section V, the data rates of the discrete channels are totaled to realize the effective throughput of the system.

The generalized equation for the throughput of the  $4 \times 4$  MIMO system is

$$\beta_t = \beta_1 + \beta_2 + \beta_3 + \beta_4 \quad (13)$$

The effective throughput of the system observed is the sum of the individual throughputs of the SISO links; therefore, the total data rate achieved was around 85 kbps, which is approximately 18 times higher than in [27].

Furthermore, the data rates declined with an increase in the spreading factor and a lesser bandwidth. The interference was null with different bandwidths with the same spreading factor. Using discrete frequencies of the same channel provided additional degrees of freedom.

### D. Current Consumption

The power consumption of the gateway is measured using the MX19 USB 3.0 device. For assessing the current consumed

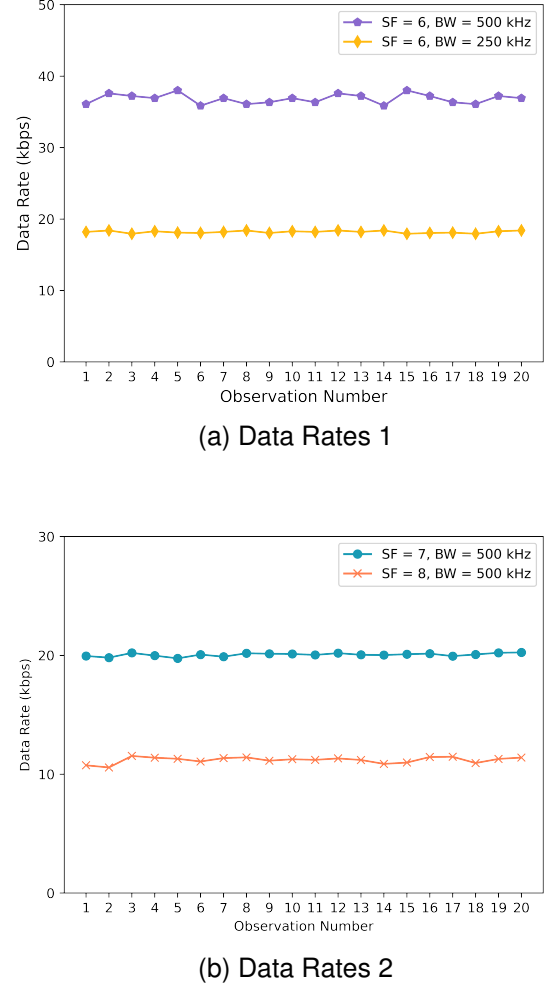


Figure 4. Throughput of LoRa module pairs

by the device, the approach sent payloads of different sizes. The payloads were strings of 40 bytes, 80 bytes, 120 bytes, 160 bytes, 200 bytes, and 240 bytes. Figure 5 illustrates the current consumed by a pair of LoRa modules with Spreading Factors 5 and 6. The current consumption raised with an increased spreading factor, as depicted in Fig V-D. There was a surge in current consumption as high as 137 mA for a pair of LoRa modules with a spreading factor of 8 while the payload size of 240 bytes. The dotted line depicts the mean current consumed by the device. When idle, the transmitter consumed 45 mA for a pair of LoRa modules, and while the receiver module was active, it drew 80 mA of current.

The current consumption is plotted for different payload sizes and spreading factors. The pairs of LoRa modules were assigned different spreading factors and bandwidth configurations.

### E. Memory Consumption

For every round, the recorded free memory ( $M_{idle}$ ) before execution helps calculate the memory consumed in real time. Then after executing the program, we recorded the available memory in the processor ( $M_{avi}$ ). The used memory is

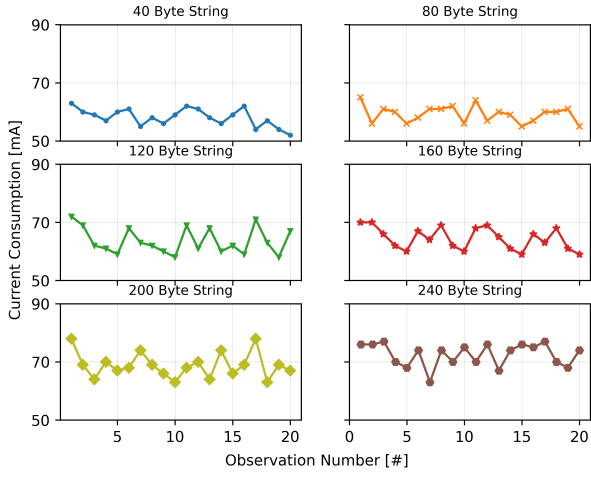


Figure 5. Current Consumed for Spreading Factors 5 and 6

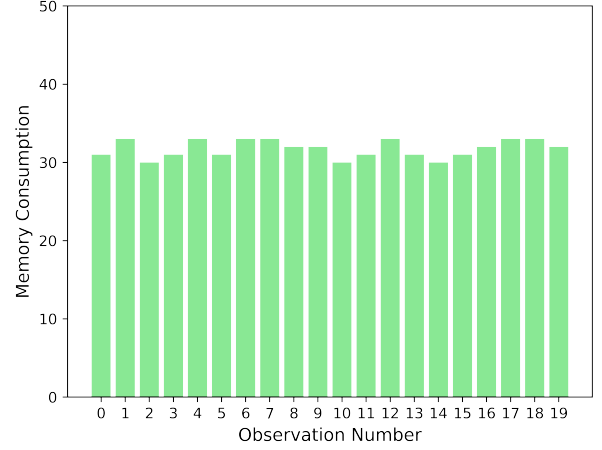


Figure 7. Memory Consumption on the MCU

$(M_{used}) = (M_{idle}) - (M_{avil})$ . The edge device consumed only 32% of the total memory for the execution of the algorithm.

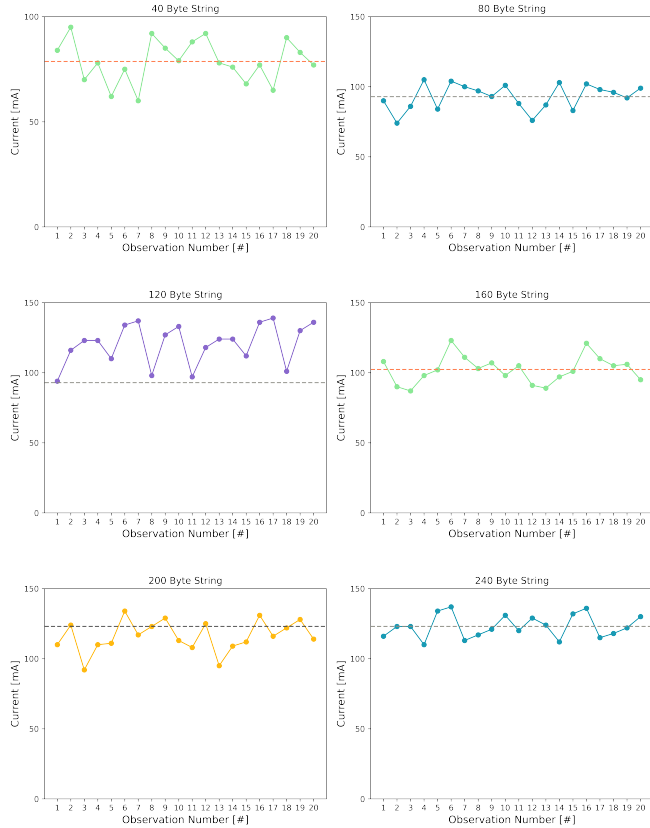


Figure 6. Current Consumed for Spreading Factors 7 and 8

## VI. CONCLUSION

The LoRa MIMO system proposed in this article addresses the throughput limitation of LoRa. The method integrates multiple-input-multiple-output with a LoRa system. We derived the expressions to evaluate the performance of the design. We demonstrate the proposed approach on a hardware test bench, verify the numerical results for enhanced throughput and channel performance, and present the resources consumed by the edge device. The presented framework is generic and relevant to a plethora of IoT deployments.

In our future work, we plan to adopt different modulation schemes, such as FSK and GFSK, and introduce precoding and decoding, to enhance the system's robustness and throughput, improving the link's reliability. There is further scope to deduce probabilistic models for allocating modulation parameters to optimize the performance of LoRa implementations.

## REFERENCES

- [1] A. Pagano, D. Croce, I. Tinnirello, and G. Vitale, "A survey on lora for smart agriculture: Current trends and future perspectives," *IEEE Internet of Things Journal*, vol. 10, no. 4, pp. 3664–3679, 2023.
- [2] H. H. R. Sherazi, L. A. Grieco, M. A. Imran, and G. Boggia, "Energy-efficient lorawan for industry 4.0 applications," *IEEE Transactions on Industrial Informatics*, vol. 17, no. 2, pp. 891–902, 2021.
- [3] B. Su, Z. Qin, and Q. Ni, "Energy efficient uplink transmissions in lora networks," *IEEE Transactions on Communications*, vol. 68, no. 8, pp. 4960–4972, 2020.
- [4] F. Benkhelifa, Z. Qin, and J. A. McCann, "User fairness in energy harvesting-based lora networks with imperfect sf orthogonality," *IEEE Transactions on Communications*, vol. 69, no. 7, pp. 4319–4334, 2021.
- [5] K. Hu, C. Gu, and J. Chen, "Ltrack: A lora-based indoor tracking system for mobile robots," *IEEE Transactions on Vehicular Technology*, vol. 71, no. 4, pp. 4264–4276, 2022.
- [6] J. Finnegan, R. Farrell, and S. Brown, "Analysis and enhancement of the lorawan adaptive data rate scheme," *IEEE Internet of Things Journal*, vol. 7, no. 8, pp. 7171–7180, 2020.
- [7] V. Toro-Betancur, G. Premasankar, C.-F. Liu, M. Slabicki, M. Bennis, and M. D. Francesco, "Learning how to configure lora networks with no regret: A distributed approach," *IEEE Transactions on Industrial Informatics*, vol. 19, no. 4, pp. 5633–5644, 2023.

- [8] H.-C. Lee and K.-H. Ke, "Monitoring of large-area iot sensors using a lora wireless mesh network system: Design and evaluation," *IEEE Transactions on Instrumentation and Measurement*, vol. 67, no. 9, pp. 2177–2187, 2018.
- [9] A. Soto-Vergel, L. Arismendy, R. Bornacelli-Durán, C. Cardenas, B. Montero-Arévalo, E. Rivera, M. Calle, and J. E. Candeló-Becerra, "Lora performance in industrial environments: Analysis of different adr algorithms," *IEEE Transactions on Industrial Informatics*, vol. 19, no. 10, pp. 10501–10511, 2023.
- [10] M. A. Karabulut, A. F. M. S. Shah, and H. Ilhan, "A novel mimo-ofdm based mac protocol for vanets," *IEEE Transactions on Intelligent Transportation Systems*, vol. 23, no. 11, pp. 20255–20267, 2022.
- [11] T. Elshabrawy and J. Robert, "Capacity planning of lora networks with joint noise-limited and interference-limited coverage considerations," *IEEE Sensors Journal*, vol. 19, no. 11, pp. 4340–4348, 2019.
- [12] G. Zhu, C.-H. Liao, T. Sakdejayont, I.-W. Lai, Y. Narusue, and H. Morikawa, "Improving the capacity of a mesh lora network by spreading-factor-based network clustering," *IEEE Access*, vol. 7, pp. 21584–21596, 2019.
- [13] P. Edward, M. El-Aasser, M. Ashour, and T. Elshabrawy, "Interleaved chirp spreading lora as a parallel network to enhance lora capacity," *IEEE Internet of Things Journal*, vol. 8, no. 5, pp. 3864–3874, 2021.
- [14] P. Kumari, H. P. Gupta, and T. Dutta, "An incentive mechanism-based stackelberg game for scheduling of lora spreading factors," *IEEE Transactions on Network and Service Management*, vol. 17, no. 4, pp. 2598–2609, 2020.
- [15] ———, "Estimation of time duration for using the allocated lora spreading factor: A game-theory approach," *IEEE Transactions on Vehicular Technology*, vol. 69, no. 10, pp. 11090–11098, 2020.
- [16] D. Croce, M. Gucciardo, S. Mangione, G. Santaromita, and I. Tinnirello, "Lora technology demystified: From link behavior to cell-level performance," *IEEE Transactions on Wireless Communications*, vol. 19, no. 2, pp. 822–834, 2020.
- [17] F. Benkhelifa, Y. Bouazizi, and J. A. McCann, "How orthogonal is lora modulation?" *IEEE Internet of Things Journal*, vol. 9, no. 20, pp. 19928–19944, 2022.
- [18] L. Amichi, M. Kaneko, N. E. Rachkidy, and A. Guitton, "Spreading factor allocation strategy for lora networks under imperfect orthogonality," in *ICC 2019 - 2019 IEEE International Conference on Communications (ICC)*, 2019, pp. 1–7.
- [19] A. Waret, M. Kaneko, A. Guitton, and N. El Rachkidy, "Lora throughput analysis with imperfect spreading factor orthogonality," *IEEE Wireless Communications Letters*, vol. 8, no. 2, pp. 408–411, 2019.
- [20] Q. Zhang, I. Bizon, A. Kumar, A. B. Martinez, M. Chafii, and G. Fettweis, "A novel approach for cancelation of nonaligned inter spreading factor interference in lora systems," *IEEE Open Journal of the Communications Society*, vol. 3, pp. 718–728, 2022.
- [21] R. Narayanan, S. Kumar, and C. S. R. Murthy, "Cross technology distributed mimo for low power iot," *IEEE Transactions on Mobile Computing*, vol. 21, no. 5, pp. 1609–1624, 2022.
- [22] J.-M. Kang, "Mimo-lora for high-data-rate iot: Concept and precoding design," *IEEE Internet of Things Journal*, vol. 9, no. 12, pp. 10368–10369, 2022.
- [23] H. Ma, G. Cai, Y. Fang, P. Chen, and G. Han, "Design and performance analysis of a new stbc-mimo lora system," *IEEE Transactions on Communications*, vol. 69, no. 9, pp. 5744–5757, 2021.
- [24] D. Croce, M. Gucciardo, S. Mangione, G. Santaromita, and I. Tinnirello, "Lora technology demystified: From link behavior to cell-level performance," *IEEE Transactions on Wireless Communications*, vol. 19, no. 2, pp. 822–834, 2019.
- [25] J.-T. Lim and Y. Han, "Spreading factor allocation for massive connectivity in lora systems," *IEEE Communications Letters*, vol. 22, no. 4, pp. 800–803, 2018.
- [26] J. Niu, X. Yang, S. Liu, Y. Li, and Y. Guo, "Energy-efficient adaptive virtual-mimo transmissions for lora uplink systems," *Digital Signal Processing*, vol. 127, p. 103493, 2022.
- [27] H. Pirayesh, S. Zhang, P. K. Sangdeh, and H. Zeng, "Maloragw: Multi-user mimo transmission for lora," in *Proceedings of the 20th ACM Conference on Embedded Networked Sensor Systems*, ser. SenSys '22. New York, NY, USA: Association for Computing Machinery, 2023, p. 179–192. [Online]. Available: <https://doi.org/10.1145/3560905.3568533>